

1N-39
14444
P16

Simulation of Probabilistic Wind Loads and Building Analysis

Ashwin R. Shah
Sverdrup Technology, Inc.
Lewis Research Center Group
Brook Park, Ohio

and

Christos C. Chamis
National Aeronautics and Space Administration
Lewis Research Center
Cleveland, Ohio

Prepared for the
Ninth Biennial Conference on Reliability, Stress Analysis, and Failure Prevention
sponsored by the American Society of Mechanical Engineers
Miami, Florida, September 22 - 25, 1991

NASA

(NASA-TM-103744) SIMULATION OF
PROBABILISTIC WIND LOADS AND BUILDING
ANALYSIS (NASA) 16 p

CSC 20K

N91-23549

Unclass
0014444

G3/39

SIMULATION OF PROBABILISTIC WIND LOADS AND BUILDING ANALYSIS

Ashwin R. Shah
Sverdrup Technology, Inc.
Lewis Research Center Group
Brook Park, Ohio 44142

and

Christos C. Chamis
National Aeronautics and Space Administration
Lewis Research Center
Cleveland, Ohio 44135

ABSTRACT

Probabilistic wind loads likely to occur on a structure during its design life are predicted. This report describes a suitable multifactor interactive equation (MFIE) model and its use in the Composite Load Spectra (CLS) computer program to simulate the wind pressure cumulative distribution functions on four sides of a building. The simulated probabilistic wind pressure load was applied to a building frame, and cumulative distribution functions of sway displacements and reliability against overturning were obtained by using NESSUS (Numerical Evaluation of Stochastic Structure Under Stress), a stochastic finite-element computer code. The geometry of the building and the properties of building members were also considered as random in the NESSUS analysis. The uncertainties of wind pressure, building geometry, and member section property were quantified in terms of their respective sensitivities on the structural response.

INTRODUCTION

Any structure built on the Earth is subjected to natural and unnatural loads. Wind constitutes a major form of natural load on a structure. Determining wind loads requires the prediction of the magnitudes and directions of wind speeds and respective pressures on a structure's surfaces. Predictions of wind speed and its flow around complicated structures are at best estimates. According to McDonald (1975), the process of estimating wind loads on buildings involves a relatively large number of unknowns, and it is difficult to formulate relationships among them and to account for the associated uncertainties. Therefore, analysis and design of building structures should account for uncertainties in the wind loads as well as in building structural parameters in order to quantify the structure's reliability for its design life.

In light of the difficulties and uncertainties associated with wind loads and structural parameters, a formal methodology is required to probabilistically simulate the corresponding uncertainties in the structural response. A multifactor interactive equation (MFIE) (Boyce and Chamis, 1988) was adapted in this investigation to computationally simulate the probabilistic wind loads on a building (Fig. 1); it was used in conjunction with the Composite Load Spectra (CLS) computer code (Newell et al., 1986). CLS was developed by the NASA Lewis Research Center to simulate probabilistic composite loads on components of the space shuttle main engine (SSME). The simulation of probabilistic loads in CLS involves identifying primitive variables and their relationship. The atmospheric pressure and temperature, the roughness of the terrain, and the frequency content and duration of gusts are related to wind load by MFIE. The frequency content and duration of gusts were included to account for

the short-duration gust effect. The effect of a gust is to amplify the pressures on a building. The cumulative distribution functions (CDF) for wind pressures on four sides of a building due to mean wind directions of 0° and 45° to the building face were simulated in order to study the effect of wind direction on the sway response and stability of the building.

A probabilistic structural analysis of a building frame subjected to the simulated probabilistic wind pressure loads together with the uncertainties of building geometry, member section properties, and material properties was performed by using NESSUS (a stochastic finite-element computer code entitled "Numerical Evaluation of Stochastic Structure Under Stress" developed at the NASA Lewis Research Center) (SRI, 1989). The CDF's of maximum sway displacements at the top of the building and the reliability against overturning were computed. Probability distributions of the forces in a typical building member, which are required to design the member itself and the connections between members, were obtained. The effect of random wind direction on the building responses was also studied. A hierarchy of the sensitivity of the primitive variables to the response variable was established.

STRUCTURE OF CLS

The computer code CLS simulates the probabilistic centrifugal, pressure, thermal, and other loads for SSME aerospace components such as the turbine blades, the liquid oxygen post, and the transfer duct. The input required to simulate loads is the primitive variables, their statistical distributions, and the number of bins required to discretize the input probability density function (PDF). The process of simulating load uncertainties is based on the influence coefficient model for a particular load type. The influence coefficient model defines the physics of the load process in the form of a primitive variables relationship. Therefore, a different influence coefficient model is required for each load type. For the case of wind a multifactor interactive equation model, as discussed later, was adapted to simulate the wind speeds and pressures on four sides of a building.

The MFIE model and the probabilistic load simulation method (Newell et al., 1986; and Kurth, 1985) available in CLS were used to simulate the CDF's of wind speeds and pressures on building surfaces. The input primitive variables were discretized into discrete probability distributions by using either equal or unequal probability intervals. The unequal probability interval option can be used effectively to achieve more accurate distribution of dependent variables in the tail regions. Random samples of primitive variables within the number of discrete intervals were generated and combined by MFIE to calculate wind speed. The wind speed was then transformed into an equivalent pressure force on each face of the building. Several ordered pairs of pressure forces were obtained. A condensation procedure (Kurth, 1985) was used on these pairs to obtain the CDF's of pressure forces on the buildings. The details of this process are given later.

STRUCTURE OF NESSUS

NESSUS is an integrated, advanced, probabilistic, finite-element analysis computer code for performing static, dynamic, buckling, and nonlinear analyses. NESSUS consists of three major modules; NESSUS/PRE, NESSUS/FEM, and NESSUS/FPI. The general form of the input for any structural analysis problem involves identifying primitive variables and their statistical distributions, structural geometry, loads, boundary conditions, etc. The three major NESSUS modules are described briefly here.

NESSUS/PRE is a preprocessor used to analyze and prepare statistical data needed to perform the probabilistic finite-element analysis. NESSUS/PRE decomposes any

Gaussian-correlated random field defined at discrete finite-element nodes into a set of uncorrelated independent vectors by using modal analysis.

NESSUS/FEM is a general-purpose, finite-element code that uses the perturbation algorithm to perform structural analysis and to evaluate the sensitivity due to variation in uncorrelated primitive variables. A modified version of Newton's nonlinear algorithm is used to perform the perturbation analysis. A discrete representation of the response surface required for probabilistic analysis in NESSUS/FPI is obtained by perturbing independent random variables.

NESSUS/FPI has several reliability algorithms, such as fast Monte-Carlo simulation, fast probability integration, and first-order and second-order reliability analysis. The fast probability integration algorithms is efficient and gives accurate results even in the lower and upper probability regions. NESSUS/FPI extracts the data base created by NESSUS/FEM and develops an explicit response function. The fast probability integration is performed by using the explicit response function together with statistical distributions of primitive variables. The NESSUS/FPI output contains the CDF of the response and the quantified primitive variable uncertainties in the form of sensitivity.

MFIE MODEL FOR WIND

The evolution of an MFIE model for wind loads is based on a generic material behavior MFIE model (Boyce and Chamis, 1988) used for structural analysis. The MFIE model for wind was adapted, by using similar concepts and guidelines, to simulate wind speed from the constituent primitive variables. Wind speed has two parts, static and dynamic. The atmospheric pressure, the temperature, and the roughness of the terrain normally contribute to the static wind speed. In order to account for occasional high speeds, it is necessary to include the dynamic part of the wind. The dynamic part is the turbulence caused by gusts. A gust is a short-duration effect and is normally characterized by its frequency content and its duration. The effect of a gust is to substantially amplify the magnitude of the wind speed. Thus, the effect of gusts is included in an implicit way in the MFIE model for wind speed through their frequency content and duration. The general form of the model is

$$\frac{S}{S_0} = \left(\frac{P_f - P}{P_f - P_0} \right)^a \left(\frac{T_f - T}{T_f - T_0} \right)^b \left(\frac{R_f - R}{R_f - R_0} \right)^c \left(\frac{\omega_f - \omega}{\omega_f - \omega_0} \right)^d \left(\frac{t_f - t}{t_f - t_0} \right)^e \quad (1)$$

where

S	wind speed, mph
P	atmospheric pressure, psi
T	atmospheric temperature, °F
R	roughness of terrain, ft
ω	frequency content of gust, Hz
t	duration of gust, sec
a,b,c,d,e	exponents

and the variables with subscript 0 represent the reference conditions and those with f represent the final condition of the variable.

The exponents a, b, c, d, and e can be determined through a regression analysis of the actual data, or in the absence of data they can be selected probabilistically from ranges estimated by expert opinion.

All the variables in equation (1) including the exponents can be random with any distribution. In the present case all the variables were assumed to have normal distribution. Their mean and standard deviations are given in Table I.

WIND LOAD SIMULATION

The CLS program was modified to incorporate the MFIE model for wind load simulation. Several options for the MFIE model, such as computation of static wind speed, dynamic (gust) wind speed, and wind pressure are provided in the code. Wind load primitive variable uncertainties were simulated by combining the MFIE model and the random sampling condensation algorithm in CLS. Its procedural details are given here.

For every sample of the primitive variables the wind speed was calculated by using equation (1). The computed wind speed was decomposed into two components normal to the appropriate building surfaces for the sampled wind direction with respect to the X axis (Fig. 2). From these components and the respective pressure coefficients C_p the wind pressure on all the sides of the building was computed by the following equation (McDonald, 1975):

$$\text{Pressure} = 0.012873 C_p S^2 \text{ (lb/ft}^2\text{)} \quad (2)$$

The pressure coefficients on four sides of the building due to wind from different directions are given in Fig. 3 (McDonald, 1975). The pressure induced by the wind speed components on a given face were added to obtain the total pressure. Although the variation in pressure along the height was neglected, it can be considered and the CDF of the pressure at different heights can also be calculated.

Two specific cases of wind load simulation were evaluated: (1) the sensitivity of the MFIE exponents to wind speed and (2) the computation of wind pressures on the faces of a multistory building. Sensitivity is defined as the change in the wind speed CDF due to the change in the mean value of a particular exponent while its coefficient of variation and the distributions of other primitive variables are kept the same. The sensitivity of the static wind speed CDF to the atmospheric pressure and temperature exponents is shown in Figs. 4 and 5, respectively. The sensitivity of the static wind speed mean and standard deviation to the atmospheric pressure and temperature exponents is given in Figs. 6 and 7, respectively.

The wind pressure CDF on the building faces was simulated for two cases: The mean angle of wind direction was assumed to be the positive X axis (Fig. 2); the mean angle of wind direction was assumed to be at a 45° angle to the X axis toward the positive Z axis (Fig. 2). The primitive variables, their distribution types, and the parameters used to simulate wind pressures on building faces are given in Table I. The corresponding CDF's of the wind speed and pressures on all sides of the building for both cases are given in Figs. 8 and 9. These figures show that the CDF's are of the extreme-value type. It is worth noting that the suction pressure can reach 400 lb/ft² with a probability of 0.00001 (which is about 20 percent of perfect vacuum) and that the pressures on all four sides are correlated. The strength of the correlations depends mainly on the wind direction.

BUILDING FRAME ANALYSIS

The building frame (Fig. 1) was analyzed for the probabilistic wind loads simulated by MFIE and CLS (as already described) and for the uncertainties in the material properties, the member section properties, and the building geometry. The corresponding distribution of wind pressure was applied on the respective faces. Since the building was relatively short, the variation of pressure along the height was neglected. The mean value, the coefficient of variation, and the distribution of the primitive variables considered in the analysis are given in Table II. The typical live load for residential buildings of 150.0 lb/ft^2 with a coefficient of variation of 20.0 percent was assumed in this analysis. The floors were assumed to be of 4.0-in.-thick concrete. The columns and beams were assumed to be steel sections from the Manual of Steel Construction (AISC, 1980). A 5.0 percent variation in the section properties was assumed to account for the manufacturing and modeling uncertainties in the analysis. The connections between the beam columns and the column foundations were assumed to be rigid.

Normally, buildings subjected to lateral loads are prone to unacceptable levels of sway because of the serviceability requirements and to overturning from the stability point of view. Therefore, in this investigation, the CDF of lateral sway displacement and the probability of overturning were computed by using NESSUS. Also, the probability distributions of the typical member forces were obtained for the corresponding probability distributions of overturning and sway. The CDF and the sensitivity of primitive variables for axial force, shear force, moment about the Z axis, and moment about the X axis in the windward-side base column are plotted in Figs. 10 to 13, respectively. These member force distributions can be used to size the members and the connections between them. The CDF's of sway displacement for the top story of the building were obtained and are plotted in Figs. 14(a) and 15(a) for mean wind speed directions of 0° and 45° , respectively. The sensitivity of the primitive variables in these respective cases is given in Figs. 14(b) and 15(b). The resistance against overturning was derived mainly from the weight of the building, which include deadweight, live load, and the weight of the foundation, since the foundation is an integral part of the building. It was assumed in this analysis that the foundation had been properly designed against any local failure. The force distributions required to design the foundation against such local failures can be obtained from the methodology used in this study. The uncertainties associated with live load were also considered in the reliability calculation against overturning. The computed probability density functions for the overturning and resisting moments at 0° mean wind speed direction are given in Fig. 16. The probability of overturning was computed to be 63 times out of 10 000. The sensitivity of the primitive variables to the overturning moment is plotted in Fig. 17.

DISCUSSION OF RESULTS

Wind Load Simulation

Sensitivity analysis. Figures 4 to 7 show that the exponent for temperature effect was more sensitive to wind speed than that for pressure effect. The variation in the mean wind speed magnitude was affected primarily by the pressure effect exponent; the scatter was affected by the temperature effect exponent. This study can be used to decide the bounds on the exponent that will lead to a feasible model. However, verifying the model with actual data should not be ruled out.

Probabilistic analysis. The CDF of the steady-state wind speed is shown in Fig. 8(a). The steady-state wind speed range is not large. However, the CDF required for design is the one that includes the dynamic (gust) part. The CDF of the

wind speed with the dynamic part superimposed onto the static part is given in Fig. 8(b). The dynamic effect amplified the wind speed by 3 to 4 times, which conforms with the so-called pseudodynamic amplification factors used by the building industry in designing for wind loads (McDonald, 1975; and Newberry and Eaton, 1975). The steady-state mean wind obtained was 10 mph; the static plus dynamic mean wind speed was 48 mph. These CDF's are of the extreme-value type. The wind speed was converted to the equivalent dynamic pressure forces by using equation (2). In this computation the pressure coefficients were assumed to be deterministic, but they can be considered to be probabilistic also. The pressure distribution curves in Fig. 9(a) for the 0° mean wind direction show that the $-X$ face (the building face with outward normal in the $-X$ direction) experienced mainly pressure load, whereas the other faces experienced suction loads because the suction from the wind speed component in the X direction was much higher than the pressure from the wind speed component in the $-Z$ direction. However, when the mean wind speed direction was 45° (Fig. 9(b)), the Z face had samples of wind speed components that were fairly large in magnitude. Therefore, the pressure distribution on the $-X$ and Z faces varied from pressure to suction. However, the X face and the $-Z$ face remained under suction because whether the wind component was in the X direction or the $-Z$ direction the pressure coefficients for these faces were still negative.

Building frame analysis. The CDF of axial and shear force and the end moments about the Z and X axes for the base column on the windward side as shown in Figs. 10 to 13 turned out to be of the extreme-value type, a clear indication of the wind load distribution's predominance. The axial force CDF as given in Fig. 10 shows variation from compression to tension. The tensile force in the member reveals the scatter in the uplift force. From this curve it can be easily inferred that the CDF of axial force in the leeward-side column will show scatter in the compression force that can be used to design the column against buckling. Figure 10(b) clearly shows the wind load uncertainties in the upper tail to be highly sensitive, whereas at low cumulative probability levels the area of cross section, the width and height of the building, shows significant sensitivity. In case of shear force distribution, as depicted in Fig. 11, the height and width of the building and the wind pressures dominated equally at low probability levels. But again, only the windward pressures dominated the response at higher probability levels. It is evident from Fig. 12 that the moment about the Z axis in the windward-side column at higher probability levels was largely governed by many variables, such as the height of the building, the windward and leeward pressures, and the shear area of the member cross section. The moment at the higher probability levels was the positive moment, which is not mainly responsible for the overturning of the building in general. Conversely, at the lower probability levels the windward pressure was the only dominating variable to the negative moment which was responsible for the overturning. The moment about the X axis in the member (Fig. 13) was essentially governed by the wind pressures on building faces normal to the Z axis. Also, its magnitude was very low, since the distribution of wind pressure on these faces had almost the same nature and magnitude as the CDF but opposite in direction. These force distributions are a valuable and important piece of information for use in designing the members and the connections.

The distributions for the sway displacements at 0° and 45° mean wind directions were drastically different (Figs. 14 and 15). However, the absolute magnitudes of the maximum possible sway displacements were the same. The reason is that the absolute magnitudes of the pressure forces for both wind directions (Fig. 9) were very close. For the 45° wind direction the sway occurred on either side owing to the presence of suction and pressure forces in the CDF on the $-X$ face. The mean value of sway displacement at the 0° and 45° mean wind directions, 0.16 and 0.20 in., were almost of the same magnitude. The mean speed to induce these magnitudes of sway was

about 48 mph, which is a typical design value in the industry (Newberry and Eaton, 1975). The sway displacement distribution for 0° wind direction almost followed the distribution of wind pressure force for the simple reason that the wind pressure uncertainty dominated the response at all probability levels, as observed in Fig. 14(b).

For the 45° wind direction the displacement probabilities in the lower tail were governed by the windward pressure forces, and those in the upper tail by both windward and leeward pressure forces and height. Comparing the sway response CDF for both wind directions shows that the probability that absolute sway displacement would occur was higher at 45° than at 0° . However, in both the cases the wind pressure force uncertainties played an important role in the design procedure. From the sway displacement distributions, if the building had to be designed to accommodate sway magnitudes of the order of 0.8 in., the design wind speed would be of the order of 175 mph. Looking at the discussions in Eaton (1980) that the design wind speed with a cumulative probability of occurrence of 0.63 for low-income housing in the Caribbean is 111 mph, the wind speed of 175 mph for the cumulative probability of 0.99 obtained in this study sounds reasonable.

Overturning. The overturning analysis was performed for the 0° mean wind direction only. The probability density function of the overturning moment (Fig. 16) had a Weibull type of distribution that is almost same as the pressure force distribution on the windward face. The sensitivity charts show that the windward and leeward force distributions and the height and width of the building dominated the overturning moment in the lower tail, whereas the windward pressure force governed it in the upper tail. Since overturning is largely governed by the wind pressure force, the building can be made more reliable by providing a higher resisting moment. The resisting moment comes mainly from the weight of the structure and the width and depth of the foundation; therefore the designer can adjust these variables to decrease the probability of overturning.

CONCLUSIONS

A methodology to probabilistically simulate the wind loads on structures and then perform a probabilistic evaluation of a structure subjected to these simulated wind loads has been developed. The probabilistic simulation of wind load is accomplished with the aid of multifactor interaction equation (MFIE) model concepts in conjunction with the Composite Load Spectra (CLS) computer program. The probabilistic assessment of the structure subjected to stochastic wind loads is achieved by coupling the CLS computer code with the stochastic finite element program NESSUS (Numerical Evaluation of Stochastic Structures Under Stress). The methodology was demonstrated by simulating probabilistic wind loads for a multistory building and performing probabilistic structural analysis of the building by using NESSUS. The cumulative distribution functions and the quantified sensitivity information obtained from NESSUS can be used directly to assess the reliability and the risk associated with the integrity or stability of a building. Also, with this information a building can be designed for a specified reliability. The results show that for the building analyzed, the wind pressure force played the significant role in the sway and overturning behavior of the building. In short, following the concepts of MFIE model and CLS, the probabilistic wind loads for any structure can be simulated and NESSUS computer codes can be used effectively for the subsequent probabilistic assessment.

REFERENCES

- AISC, 1980, Manual of Steel Construction, Eighth Edition, American Institute of Steel Construction Inc., Chicago, IL.
- Boyce, L., and Chamis C.C., 1988, "Probabilistic Constitutive Relationships for Cyclic Material Strength Models," 29th Structures, Structural Dynamics and Materials Conference, Williamsburg, VA, Technical Papers, AIAA, Washington, D.C., pp. 1299-1306.
- Eaton, K.J., 1980, "Low-Income Housing and Hurricanes," Fifth International Conference on Wind Engineering Research, Fort Collins, CO, J.E. Cermack, ed., Pergamon Press, New York, Vol. 1, pp. 7-15.
- Kurth, R.E., 1985, "The Development and Application of a New Probabilistic Analysis Technique for Nuclear Risk Calculations," Ph.D. Thesis, The Ohio State University, Columbus, OH.
- McDonald, A.J., 1975, Wind Loading on Buildings, John Wiley & Sons, New York.
- NESSUS Users Manual, 1989, Southwest Research Institute, San Antonio, TX, NASA Contract NAS3-29389.
- Newberry, C.W., and Eaton, K.J., 1975, Wind Loading Handbook, H.M.S.O., London, England.
- Newell, J.F, Kurth, R.E., and Ho, H.W., 1986, "Composite Load Spectra for Select Space Propulsion System Components," NASA Contractor Report, NASA CR-179496.

TABLE I. - PRIMITIVE VARIABLES

FOR WIND LOAD SIMULATION

[All the primitive variables are assumed to be normally distributed.]

Primitive variable name	Mean	Standard deviation
Final pressure, psi	16.0	0.03
Current pressure, psi	14.5	0.10
Pressure exponent	5.0	1.20
Final temperature, °F	120.0	2.00
Current temperature, °F	68.0	8.00
Temperature exponent	-2.0	0.40
Final roughness, ft	30.0	1.00
Current roughness, ft	5.0	3.00
Roughness exponent	0.2	0.01
Wind direction, deg	0	20.00
Final frequency, Hz	50.0	1.00
Current frequency, Hz	20.0	5.00
Frequency exponent	-1.5	0.35
Final time, sec	100.0	3.00
Current time, sec	50.0	7.00
Time exponent	-1.5	0.35

TABLE II. - PRIMITIVE VARIABLES FOR BUILDING ANALYSIS

[The coefficient of variation for all the variables except live load and dead load is 5 percent. The coefficients of variation are 20 percent for live load and 0 percent for dead load.]

Primitive variable name	Mean value	Distribution type
Modulus of elasticity, Mpsi	29	Weibull
Width along X axis, ft	15	Normal
Width along Z axis, ft	12	↓
Height of building, ft	60	
Live load on all floors, lb/ft ²	150	
Dead load of floor slabs, lb/ft ²	50	
Section properties: ^a		Normal ↓
Columns (floors 1 to 3)	W18X71	
Columns (floors 4 and 5)	W18X60	
Beams along X axis (floors 1 and 2)	W12X58	
Beams along X axis (floors 3 to 5)	W12X50	
Beams along Z axis (floors 1 and 2)	W12X50	
Beams along Z axis (floors 3 to 5)	W12X40	

^aSection properties and notation are taken from the Manual of Steel Construction (AISC, 1980).

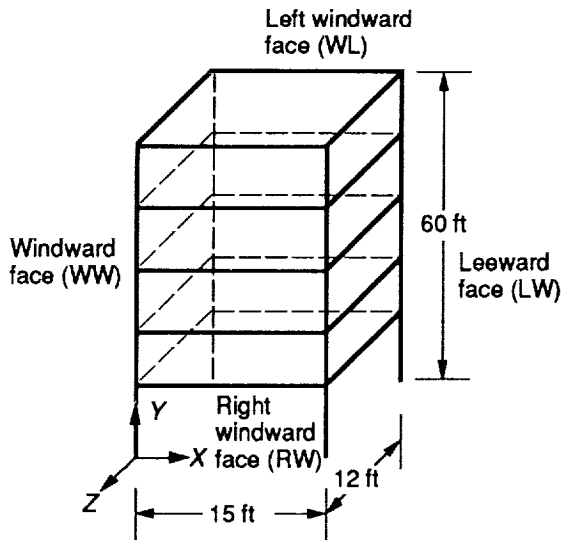


Figure 1.—Building frame.

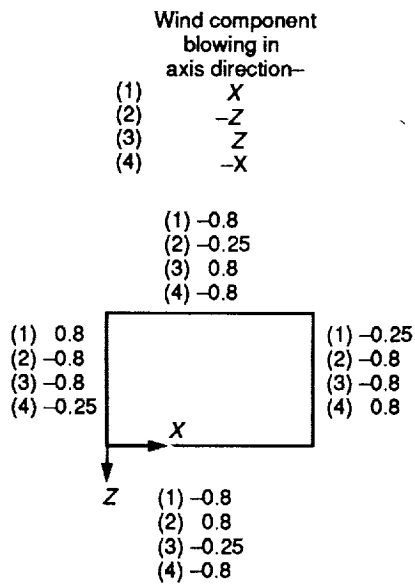


Figure 3.—Pressure coefficients on building faces.

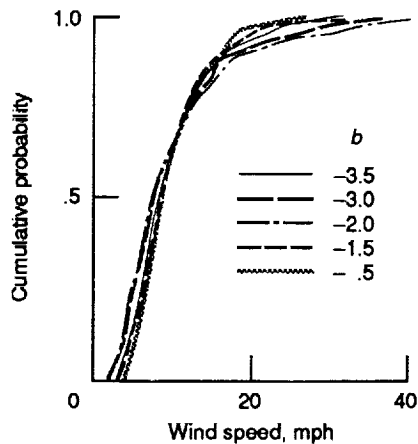


Figure 5.—Effect of variation in temperature exponent b on wind speed CDF.

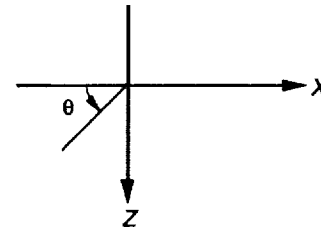


Figure 2.—Sign convention for wind direction angle.

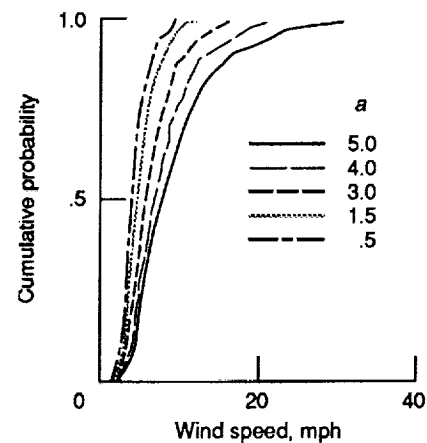


Figure 4.—Effect of variation in pressure exponent a on wind speed CDF.

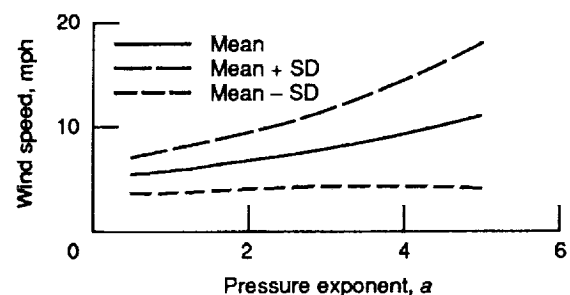


Figure 6.—Effect of variation in pressure exponent a on wind speed mean and standard deviation.

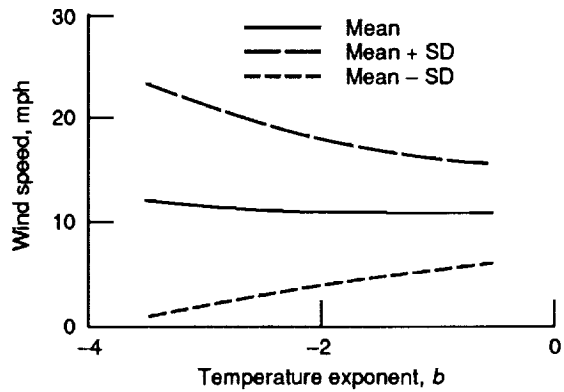


Figure 7.—Effect of variation in temperature exponent b on wind speed mean and standard deviation.

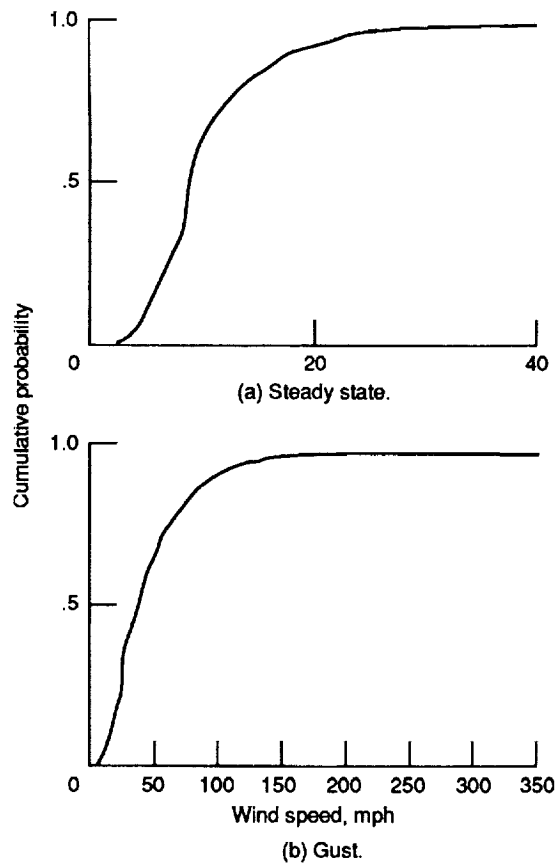


Figure 8.—Wind speed cumulative distribution functions.

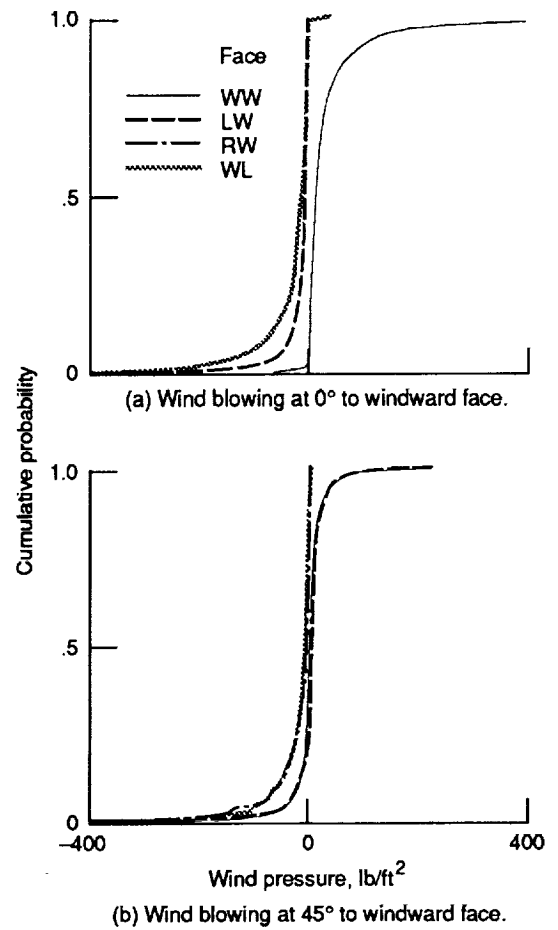
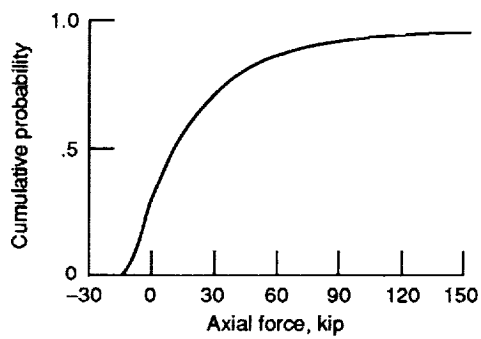
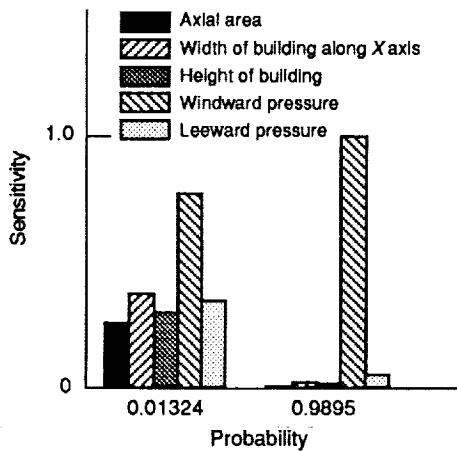


Figure 9.—Cumulative distribution function of wind pressure on building surfaces.

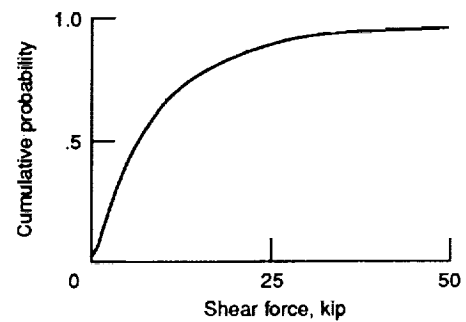


(a) Cumulative distribution function.

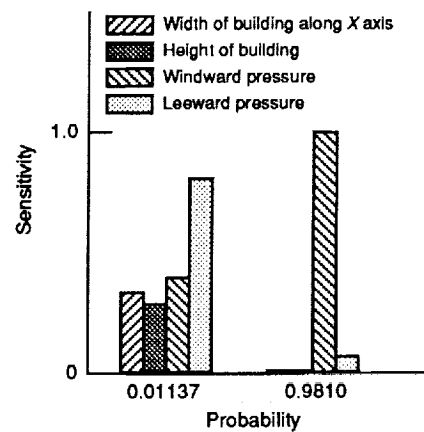


(b) Sensitivity of primitive variables.

Figure 10.—Axial force in windward-side column.

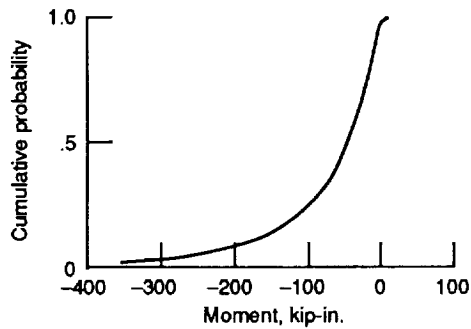


(a) Cumulative distribution function.

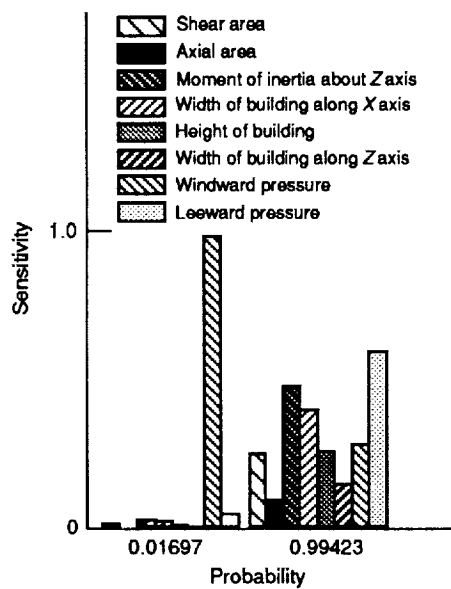


(b) Sensitivity of primitive variables.

Figure 11.—Shear force in windward-side column.

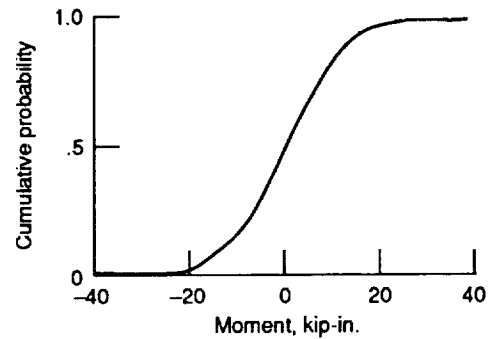


(a) Cumulative distribution function.

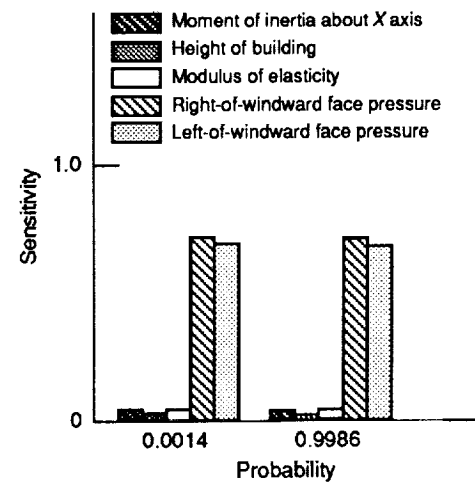


(b) Sensitivity of primitive variables.

Figure 12.—Moment about Z axis in windward-side column.

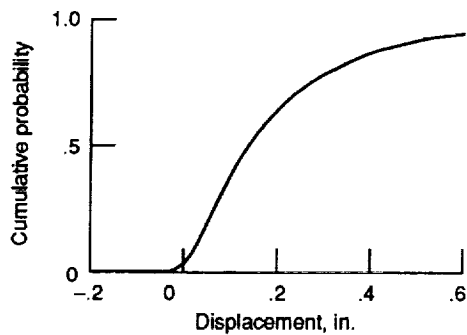


(a) Cumulative distribution function.

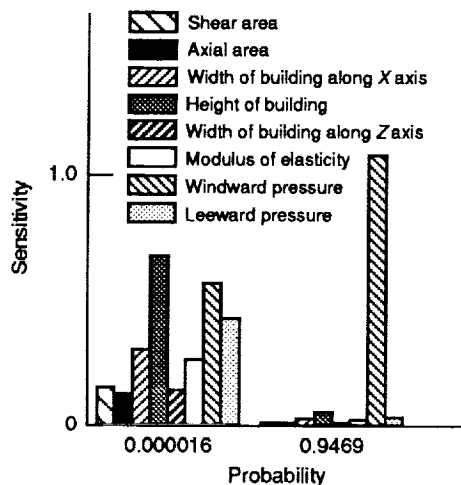


(b) Sensitivity of primitive variables.

Figure 13.—Moment about X axis in windward-side column.

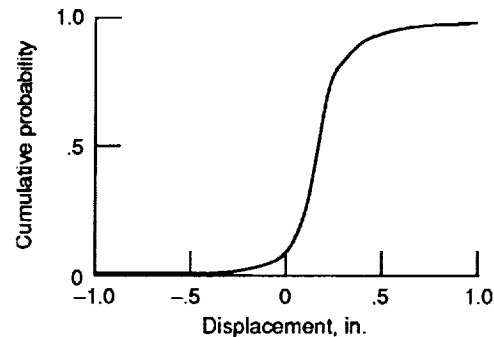


(a) Cumulative distribution function.

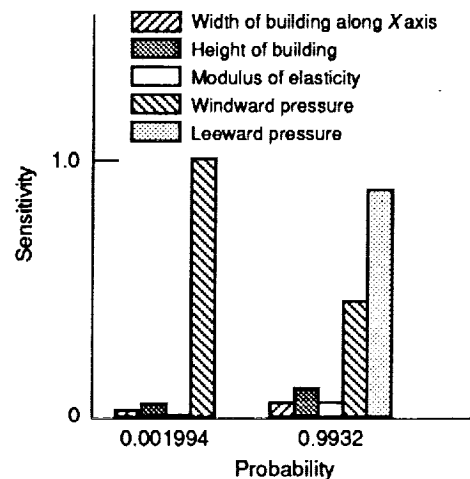


(b) Sensitivity of primitive variables.

Figure 14.—Top-story sway displacement at wind direction of 0° to windward face.



(a) Cumulative distribution function.



(b) Sensitivity of primitive variables.

Figure 15.—Top-story sway displacement at wind direction of 45° to windward face.

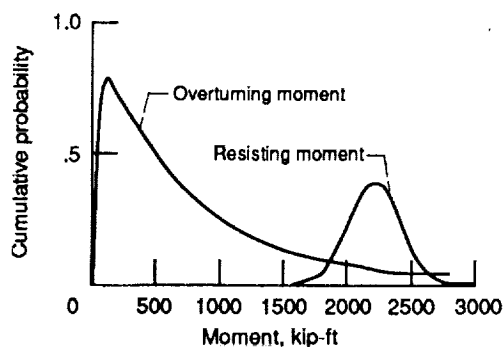


Figure 16.—Reliability against overturning.

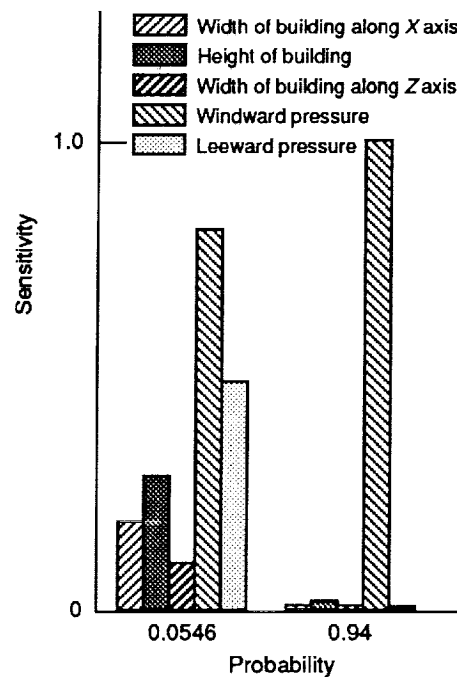


Figure 17.—Sensitivity of primitive variables to overturning moment.



National Aeronautics and
Space Administration

Report Documentation Page

1. Report No. NASA TM -103744	2. Government Accession No.	3. Recipient's Catalog No.	
4. Title and Subtitle Simulation of Probabilistic Wind Loads and Building Analysis		5. Report Date	
		6. Performing Organization Code	
7. Author(s) Ashwin R. Shah and Christos C. Chamis		8. Performing Organization Report No. E-5987	
		10. Work Unit No. 763-01-41	
9. Performing Organization Name and Address National Aeronautics and Space Administration Lewis Research Center Cleveland, Ohio 44135-3191		11. Contract or Grant No.	
		13. Type of Report and Period Covered Technical Memorandum	
12. Sponsoring Agency Name and Address National Aeronautics and Space Administration Washington, D.C. 20546-0001		14. Sponsoring Agency Code	
15. Supplementary Notes Prepared for the Ninth Biennial Conference on Reliability, Stress Analysis, and Failure Prevention sponsored by the American Society of Mechanical Engineers, Miami, Florida, September 22-25, 1991. Ashwin R. Shah, Sverdrup Technology, Inc., Lewis Research Center Group, 2001 Aerospace Parkway, Brook Park, Ohio 44142; Christos C. Chamis, NASA Lewis Research Center. Responsible person, Ashwin R. Shah, (216) 891-2263.			
16. Abstract Probabilistic wind loads likely to occur on a structure during its design life are predicted. This report describes a suitable multifactor interactive equation (MFIE) model and its use in the Composite Load Spectra (CLS) computer program to simulate the wind pressure cumulative distribution functions on four sides of a building. The simulated probabilistic wind pressure load was applied to a building frame, and cumulative distribution functions of sway displacements and reliability against overturning were obtained by using NESSUS (Numerical Evaluation of Stochastic Structure Under Stress), a stochastic finite-element computer code. The geometry of the building and the properties of building members were considered as random in the NESSUS analysis. The uncertainties of wind pressure, building geometry, and member section property were quantified in terms of their respective sensitivities on the structural response.			
17. Key Words (Suggested by Author(s)) Probabilistic; Wind; Gust; Pressure; Temperature; Roughness; Frequency; Frame; Sway; Overturning; Cumulative distribution function; Sensitivity; Reliability		18. Distribution Statement Unclassified - Unlimited Subject Category 39	
19. Security Classif. (of the report) Unclassified	20. Security Classif. (of this page) Unclassified	21. No. of pages 16	22. Price* A03

